Hindawi
Geofluids
Volume 2022, Article ID 1055463, 15 pages
https://doi.org/10.1155/2022/1055463

Research Article

Experimental Study on Reasonable Adsorption Time in Determination Coalbed Methane Content

Qiao Wang,[1,2] Zhaofeng Wang,[1,2] Jiwei Yue,[3] Liguo Wang,[1,2] Jiaxin Dong,[1,2] and Ronghui Tan[1,2]

[1]*School of Safety Science and Engineering, Henan Polytechnic University, Jiaozuo, China*
[2]*State Key Laboratory Cultivation Base for Gas Geology and Gas Control (Henan Polytechnic University), Jiaozuo, China*
[3]*School of Safety Science and Engineering, Anhui University of Science and Technology, Huainan, China*

Correspondence should be addressed to Zhaofeng Wang; zhaofengw@hpu.edu.cn and Jiwei Yue; jwyue@aust.edu.cn

Received 13 February 2022; Revised 28 February 2022; Accepted 4 March 2022; Published 1 April 2022

Academic Editor: Xuelong Li

Accurate determination of coalbed methane (CBM) content is of great significance to coalmine methane prediction, methane extraction, and gas outburst prevention. The adsorption time affects the CBM content by affecting the Langmuir adsorption constants when using the indirect method to determine the CBM content. To determine the reasonable adsorption time, representative coal samples (anthracite, lean coal, and gas-fat coal) and different destruction types (soft coal and hard coal) were selected. The experimental methods used are mercury intrusion porosimetry test, N_2 adsorption/desorption test, and methane isothermal adsorption test. The results show that the pore volume and the specific surface area obtained by the BJH method and BET model increase with increasing coal rank and destruction type. For anthracite soft and hard coal, lean soft coal, and gas-fat soft coal, the N_2 adsorption/desorption hysteresis loop is not closed when the relative pressure is low, indicating the existence of ink-bottle pores in these coal samples. For all tested coal samples, the longer the adsorption time is, the larger of coal methane adsorption capacity, Langmuir constant a, and CBM content are. The Langmuir constant b decreased with increasing the adsorption time. Under the condition that the reliability of the measured value is 85%, the reasonable adsorption times of coal samples are 28 h for anthracite, 18 h for lean coal, and 9 h for gas-fat coal. This study has practical help to improve the determination of CBM content, the prediction of coal seam gas outburst, and the development of CBM.

1. Introduction

Coalbed methane (CBM) content is not only one of the basic parameters for methane disaster prevention and methane utilization in coal mines but also a significant index for coal seam outburst danger evaluation and methane extraction effect investigation [1]. Measuring CBM content correctly is important for the safety of coal mining and CBM exploitation [2, 3]. CBM content determination methods are divided into the direct method and the indirect method [4–6]. The direct method, which consists of three compounds methane, namely, the desorbed methane, the lost methane, and the residual methane, is realized by collecting coal core or coal particles in underground or on the ground coal mine [7]. The desorbed methane and the residual methane can be accurately measured in laboratory, while the loss methane is estimated by desorption law [8]. The accuracy of the estimation of lost methane during sampling determines the quality of the total CBM content [9]. Therefore, the indirect method to measure the CBM content was used for many coal mines [10, 11]. The indirect method is realized by drilling holes in coal seam under coal mine; the coal samples drilled from the coal seam are sent to the laboratory for the determination of Langmuir adsorption constants, industrial analysis, porosity, and other parameters [6]. The Langmuir adsorption constants are one of the main factors to determine the CBM content for indirect method [12, 13].

Langmuir adsorption constant a is the maximum adsorption content when the equilibrium pressure is infinite, which represents the adsorption capacity of coal [14].

Table 1: The basic parameters of coal samples.

Coal samples	M_{ad} (%)	A_{ad} (%)	V_{ad} (%)	TRD (g/cm^3)	ARD(g/cm^3)	φ (%)	f
WYY	2.24	8.68	8.47	1.61	1.35	15.86	1.28
WYR	2.58	7.91	8.42	1.54	1.27	16.90	0.45
PY	1.53	7.14	11.84	1.43	1.28	10.35	0.56
PR	1.55	7.51	10.58	1.39	1.24	10.60	0.24
QFY	1.01	11.01	36.04	1.40	1.28	8.52	0.53
QFR	1.02	9.18	32.85	1.43	1.32	7.46	0.15

Langmuir adsorption constant b describing the intensity of the adsorption energy is the ratio of desorption rate to adsorption rate [15]. Many scholars studied the factors of Langmuir constants due to the importance of it to the accuracy of determining CBM content, such as temperature, moisture, pressure, pore structure, coal rank, destruction type, and adsorption time; meanwhile, Langmuir constants are related to the adsorption capacity of coal samples. Low temperature can promote the methane adsorption capacity of coal, and high temperature has the opposite effect [16–23]. Researches indicate that the moisture can inhibit the methane adsorption of coal, resulting in the decreasing of the Langmuir a [24–26]. The pressure is conducive to the methane adsorption; the higher the pressure, the larger the adsorption capacity and the Langmuir a [27, 28]. The smaller the particle size is, the larger the gas adsorption capacity is, and then, the larger the adsorption capacity is [29–34]. High degree of metamorphism coal which has a large amount of microporous structure and specific surface area can adsorb more methane molecules and the same law with coal destruction type [18, 21, 35]. Zhao et al. [36] investigated the effect of the adsorption contact time on the desorption characteristics of coking coal particles by using mercury intrusion, N_2 adsorption method, and methane adsorption/desorption test, and a new mathematical model of desorption under different adsorption time was proposed. Surprisingly, how the adsorption time affects the Langmuir adsorption constants and then the determination of CBM content is rarely studied.

In this paper, the representative coal quality (anthracite, lean coal, and gas-fat coal) and coal samples with different destruction types (hard coal and soft coal) are selected to measure the pore structure parameters related to methane adsorption capacity. The difference in the pore structure and the adsorption capacity of all coal samples is discussed. At the same time, the relationship between the adsorption time and the Langmuir adsorption constants is studied, and then, the reasonable adsorption times for the determination of CBM content are confirmed for different coal samples (different coal ranks and destruction types).

2. Test and Method

2.1. Material. The anthracite samples with different destruction types used in the experiment were obtained from the no. 2 coal seam of the Jiulishan coal mine in Jiaozuo Mining Area, China. The lean coal samples with different destruction types were obtained from the no. 3 coal seam of the Xinyuan coal mine in Yangquan Mining Area, China. The gas-fat coal samples with different destruction types were obtained from the no. 5 coal seam of the Panbei coal mine in Huannan Mining Area, China. The coal samples of the Jiulishan coal mine used in this study were hard coal and soft coal, which were referred to as WYY and WYR, respectively. The coal samples of the Xinyuan coal mine used in this study were hard coal and soft coal, which were referred to as PY and PR, respectively. The coal samples of the Panbei coal mine used in this study were hard coal and soft coal, which were referred to as QFY and QFR, respectively. The coal samples were ground to the appropriate quantities and sizes for each test: proximate analysis (50 g of samples; 0.074-0.2 mm particle size), methane adsorption isotherm test (200 g of samples; 0.18-0.25 mm), mercury intrusion test (20 g of samples; 3-6 mm), and N_2 adsorption/desorption test (10 g; 0.18-0.25 mm). It is noted that the coal samples should be dried by the muffle furnace first, to avoid the influence of moisture on the experimental results.

The physical parameters of coal samples testing procedures were in accordance with Chinese National Standards (GB212-200, GB/T23561.12-2010, and GB/T217-2008). The physical parameters of coal samples are shown in Table 1, which include M_{ad} (moisture), A_{ad} (ash content), V_{ad} (volatile matter), TRD (true relative density), ARD (apparent relative density), porosity (φ), and f value. The f value is called the Protodyakonov coefficient and was tested by the drop hammer method. The Protodyakonov coefficient can be used to distinguish hard coal ($f > 0.5$) from soft coal ($f < 0.5$) [37].

2.2. Mercury Intrusion and Extrusion Test. Using an AutoPore IV 9505 Micrometrics Instrument, the mercury intrusion porosimetry (MIP) test of coal samples was performed. The pore structure characteristics of experimental coal samples were obtained by analyzing the MIP curves. The pore diameter can be calculated by the Washburn equation, which is shown in Equation (1) [38].

$$P_m = \frac{4\sigma \cos\theta}{d}, \tag{1}$$

where P_m is the external pressure, N; σ is the surface tension, N/m; θ is the contact angle, °; and d is the pore diameter, m.

2.3. N_2 Adsorption/Desorption Test. The N_2 adsorption/desorption isotherm curves were obtained by using a Micrometrics ASAP2020 analyzer. The test method was based on

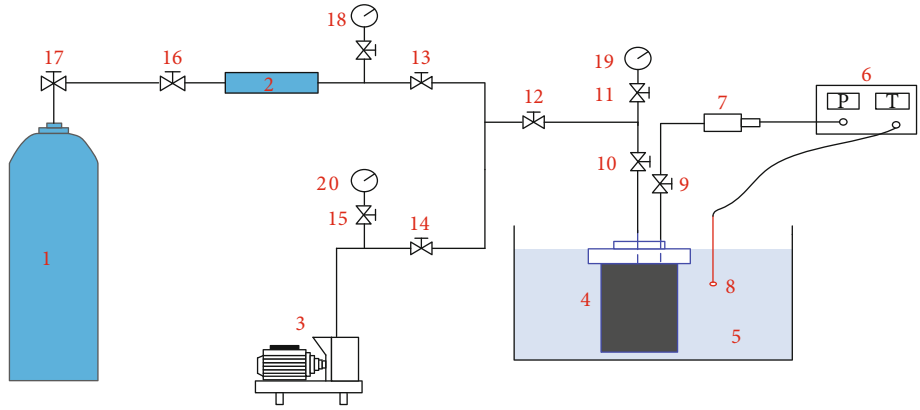

1. High pressure methane cylinder; 2. Gas tank; 3. Vacuum pump; 4. Coal sample tank; 5. Constant temperature water bath; 6. Data acquisition instrument; 7. Pressure sensor; 8. Temperature sensor; 9-17. High pressure valve; 18-19. Precision pressure gauge; 20. Vacuum gauge

Figure 1: Schematic diagram of isothermal adsorption device.

the manometric method, and the test temperature was 77 K. The specific surface area, pore volume, and pore size which analyzed by the BET model and BJH model could be obtained.

The BET model is normally used to calculate the BET surface area and is applicable for relative pressures (p/p_0) ranging from 0.05~0.35. The BJH model based on the Kelvin Equation assumes that the pore was a cylindrical model. The relationship between the pore radius and relative pressure is given by the Kelvin equation under the condition of capillary condensation.

2.4. Methane Adsorption Isotherm Test. Following the MT/T 752-1997 method for determining the methane adsorption capacity in coal (China Department of Coal Industry, 1997), the high pressure volumetric equipment was used to test the methane adsorption capacity of coal samples at 30°C. The Langmuir isotherm was drawn, and the Langmuir constants a and b were obtained. The schematic map of the methane isothermal adsorption experimental device is shown in Figure 1. The self-designed experimental device has five parts: the constant temperature water bath system, the vacuum degassing system, the methane quantitative inflation system, the adsorption equilibrium system, and the data acquisition system. The constant temperature water bath system can accurately control the coal tank temperature. The accuracy of the temperature control is ±0.01°C. The vacuum degassing system includes a vacuum gauge, a vacuum pump, and some valves. The limit vacuum of the vacuum pump is 8.0×10^{-2} Pa. The methane quantitative inflation system includes a high-pressure methane cylinder with 99.999% purity, a gas tank, and a high-precision pressure gauge which accuracy is less than 0.1% FS. The adsorption equilibrium system includes a high-precision pressure sensor, a coal sample tank, and some valves. The general experimental procedures are as shown in literature [29].

3. Test Results and Analysis

3.1. Mercury Intrusion and Extrusion Test. The pore structure in coal is complex, and many scholars have classified the pore structure according to different research objects and purposes, among which Hodot's classification is the most famous. Hodot divided the pore structure into micropores, minipores, mesopores, macropores, and visible pores, whose pore diameters are <10 nm, 10-100 nm, 100-1000 nm, 1000-100000 nm, and >100000 nm, respectively [39]. Among them, micropores mainly constitute the adsorption volume; the minipores form the space for gas diffusion and capillary condensation; the mesopores form a slow laminar permeable space; macropores constitute a strong laminar permeable space and determine the failure surface of coal with strong structural failure; visible pores form a mixture of laminar and turbulent permeability zones [34]. The Hodot's pore structure classification method was adopted in this study. The pore size distribution of coal can be measured by optical microscope, scanning electron microscope, mercury injection method, or N_2/CO_2 isothermal adsorption method. Mercury injection method is suitable for pore structure measurement with pore size larger than 5.5 nm, and compared with other methods, mercury injection method is more accurate to measure the pore size distribution of coal [32].

The MIP curves of coal samples are depicted in Figure 2. In the mercury injection stage, mercury first enters and fills the pores with larger pore sizes. With the increase of pressure, mercury enters the pores with smaller pore sizes until it reaches saturation. In the process of pressure reduction, mercury exits from the pores with smaller diameter pores first and then the larger diameter pores. As can be seen from Figure 2, for the same destruction coal type, as the metamorphic degree of coal increases, the maximum injection mercury increases, such as the WYY coal, PY coal, and QFY coal are 1.1031 mL/g, 0.0788 mL/g, and 0.0565 mL/g, respectively. And the WYR coal, PR coal, and QFR coal are 0.0704 mL/g, 0.0545 mL/g, and 0.0508 mL/g, respectively, which are shown in Table 2. For the same metamorphic degree coal, the injection mercury of hard coal is significantly greater than that of soft coal, indicating that the volume of macropores of hard coal is larger than that of soft coal.

The total pore space in coal particles is composed of effective space and isolated space. The former is the pore into which fluid can enter, and the latter is the fully closed

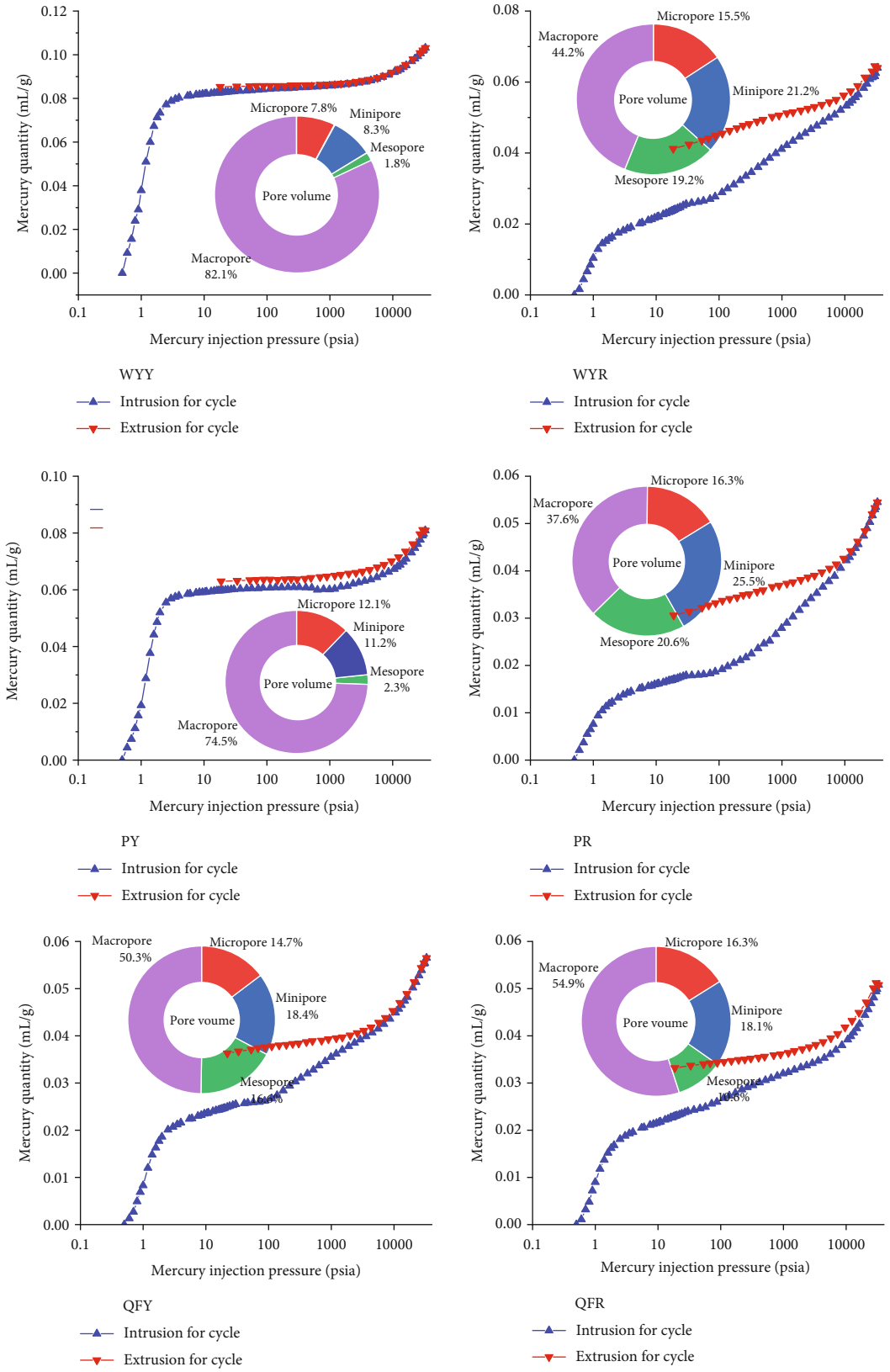

Figure 2: Mercury injection curves of coal samples.

Table 2: Fractal dimension result of coal samples.

Coal samples	$p/p_0 < 0.5$			$p/p_0 > 0.5$		
	K	D_1	R^2	K	D_2	R^2
WYY	-0.615	2.385	0.95	-0.273	2.727	0.975
WYR	-0.777	2.782	0.96	-0.218	2.23	0.97
PY	-0.64	2.36	0.96	-0.36	2.64	0.998
PR	-0.451	2.549	0.97	-0.311	2.689	0.985
QFY	-0.67	2.33	0.90	-0.55	2.45	0.988
QFR	-0.5	2.5	0.97	-0.43	2.57	0.985

"dead pore." There are three basic types of effective pores in coal: open pore, semiclosed pore, and ink-bottle pore. Mercury injection method is used to measure the pore volume of effective pores. The connectivity of pore and basic form can be evaluated by the pore hysteresis loop characteristics of mercury injection curves [31]. The mercury injection and extrusion hysteresis loop appears in open pores and thin ink-bottle pore, but a "sudden drop type" hysteresis of mercury withdrawal curve in ink-bottle pore. Due to the pressure of injection and extrusion is the same, the semiclosed pore does not have hysteresis loop.

As is shown from Figure 2, there is little hysteresis loop in WYY coal sample, which indicates that the poor connectivity of pore in WYY and the pore volume percentage of macro pores reach 82.1%. However, there is a prominent hysteresis loop in WYR coal sample, which indicates that the well connectivity of pore in WYR and the pore volume percentage of macropores and micropores reach 44.2% and 15.5%, respectively. Compared with hard lean coal PY, the pore connectivity of soft lean coal PR is obviously improved, mainly the connectivity of macropores and mesopores. As shown in Table 3, the porosity of the coal samples is as follows: WYY coal, WYR coal, PY coal, PR coal, QFY coal, and QFR coal are 81%, 52%, 67%, 46%, 45%, and 42%, respectively, which indicates that the higher the metamorphism degree of coal, the greater the total pore volume and porosity of coal. The pore volume and porosity of hard coal are higher than that of soft coal; this is because the volume of macropores and visible pores of hard coal is higher than that of soft coal. The total pore volume of hard coal is larger than that of soft coal, but the micropore volume and the percentage of micropore volume of hard coal are smaller than that of soft coal. Compared with hard coal, soft coal has more micropores and more developed pore structure, which is as shown from Figure 2.

3.2. N_2 Adsorption/Desorption Test. Adsorbed gas is mainly stored in micropore; pore characteristics of micropores have a controlling effect on methane adsorption and diffusion. Due to the mercury injection method is incomplete in the determination of specific surface area, pore volume, and other characteristics of micropores, the N_2 adsorption/desorption method is used to determine the pore structure of micropores, which can measure the aperture range is from 1.9 nm to 400 nm.

Figure 3 shows the N_2 adsorption/desorption isotherms of different destruction types with different metamorphic coal samples. As shown in Figure 3, for anthracite, lean coal, or gas fat coal sample, the adsorption capacity of soft coal is larger than the hard coal. The adsorption capacity of the coal samples increases by the following order: WYR, PR, QFR, WYY, PY, and QFY. The adsorption capacity increases with increasing destruction types and degree of metamorphism.

The adsorption isotherms were classified into six types based on IUPAC (International Union of Pure and Applied Chemistry) guidelines. The N_2 adsorption/desorption isotherm curves for the coal samples WYR, PR, and QFR are type I-B, and the coal samples WYY, PY, and QFY are type II. All coal samples contain continuous pore systems, which conclude micropore, minipore, mesopore, and macropore. There are three pore types, opened pores, semiclosed pores, and ink-bottle pore. As shown in Figure 3, all the N_2 adsorption/desorption isotherm curves exhibit hysteresis, which is the comprehensive reflection of different structure of coal samples. The closure point of adsorption hysteresis ring of many adsorbents is between 0.42 and 0.5 relative pressure, and the pore size is between 3.4 and 4.0 nm, which is calculated by Kelvin formula, namely, Equation (4). There are several reasons for adsorption hysteresis. First, the relative pressure of desorption is lower than that of adsorption, due to the difference of contact angle during adsorption/desorption process. Second, the formation modes of adsorbed and desorbed meniscus surface are different. Third, the existence of ink-bottle pores in adsorbent may result in this situation. Fourth, the N_2 molecules are trapped by the adsorption potential and cannot be released [31].

All coal samples have ink-bottle pores, but WYY coal sample is an exception. WYR, WYY, and PR coal samples are dominated by opened pores, and PY, QFY, and QFR coal samples are dominated by semiclosed pores and ink-bottle pores which cannot cause the adsorption hysteresis. It indicates that the pore connectivity of WYR, WYY, and PR coal samples is better than that of PY, QFY, and QFR coal samples. The adsorption hysteresis loops have four types, namely, H_1, H_2, H_3, and H_4. The hysteresis loop coal samples of WYY, WYR, and PR belong to H_4 type; the coal samples of PY, QFY, and QFR belong to H_3 type, which shows that some narrow slit-like pores exist in WYY, WYR, and PR coal samples.

The total specific surface area and the pore volume of coal samples with different destruction types were measured by BET model and BJH method, and the results are shown in

Table 3: Pore size parameters of coal samples.

Coal samples	Pore type	Pore size (nm)	Pore volume (mL/g)	Pore volume percentage (%)	Total pore volume (mL/g)	Porosity (%)
WYY	Visible pore	>100000	0.0713	69.16%	0.1031	81%
	Macropore	1000-100000	0.0133	12.90%		
	Mesopore	100-1000	0.0019	1.84%		
	Minipore	10-100	0.0086	8.34%		
	Micropore	5.5-10	0.0080	7.76%		
WYR	Visible pore	>100000	0.0159	22.59%	0.0704	52%
	Macropore	1000-100000	0.0152	21.59%		
	Mesopore	100-1000	0.0135	19.18%		
	Minipore	10-100	0.0149	21.16%		
	Micropore	5.5-10	0.0109	15.48%		
PY	Visible pore	>100000	0.0486	61.68%	0.0788	67%
	Macropore	1000-100000	0.0101	12.82%		
	Mesopore	100-1000	0.0018	2.29%		
	Minipore	10-100	0.0088	11.17%		
	Micropore	5.5-10	0.0095	12.06%		
PR	Visible pore	>100000	0.0119	21.83%	0.0545	46%
	Macropore	1000-100000	0.0086	15.78%		
	Mesopore	100-1000	0.0112	20.55%		
	Minipore	10-100	0.0139	25.50%		
	Micropore	5.5-10	0.0089	16.33%		
QFY	Visible pore	>100000	0.0177	31.33%	0.0565	45%
	Macropore	1000-100000	0.0107	18.94%		
	Mesopore	100-1000	0.0094	16.64%		
	Minipore	10-100	0.0104	18.41%		
	Micropore	5.5-10	0.0083	14.69%		
QFR	Visible pore	>100000	0.0162	31.89%	0.0508	42%
	Macropore	1000-100000	0.0117	23.03%		
	Mesopore	100-1000	0.0054	10.63%		
	Minipore	10-100	0.0092	18.11%		
	Micropore	5.5-10	0.0083	16.34%		

Table 4. The total pore volume increases correspondingly with increasing destruction type for the same coal rank, which results in the methane adsorption space increases with increasing destruction type. This phenomenon relates to the fact that the micropores, minipores, and mesopores were changed more by tectonic deformation. The micropores, minipores, mesopores, and the total specific surface areas increase with increasing destruction type, which is shown as Table 4 and Figure 4(a). Micropores contributed the most to specific surface area, followed by mesopores and then macropores for all coal samples. However, mesopores contributed the most to pore volume, followed by macropores and then micropores for all coal samples in N_2 adsorption/desorption test, which is shown in Figure 4(b). The average pore diameter of soft coal sample is larger than the hard coal sample and increases with increasing degree of coal metamorphism, which is shown in Table 4.

The pore fractal dimension of the coal sample is an important parameter describing the degree of the pore complexity, which can be obtained by the N_2 adsorption method. The methods for determination of the fractal dimension of coal pores include the Langmuir model, BET model, and FHH (Frenkel-Halsey-Hill) model; among them, the FHH model which is shown in Equation (2) is the mostly used [38].

$$\ln\left(\frac{V}{V_0}\right) = (D-3)\ln\left[\ln\left(\frac{p_0}{p}\right)\right] + C, \tag{2}$$

where p is the adsorption equilibrium pressure, MPa; V is the volume of gas molecules that are absorbed under the equilibrium pressure p, mL/g; V_0 is the adsorption volume of the monolayer, mL/g; p_0 is the saturated vapor pressure, MPa; D is the pore fractal dimension; and C is the fitted constants.

By the scatter plot of $\ln[\ln(p_0/p)]$ and $\ln V$ and fitting the scatter points, the slope $\boldsymbol{K}$ of the fitted line can be obtained, and the fractal dimension $\boldsymbol{D}$ can be obtained by $D = 3 + K$ (Table 2). Figure 5 shows the fitted curves

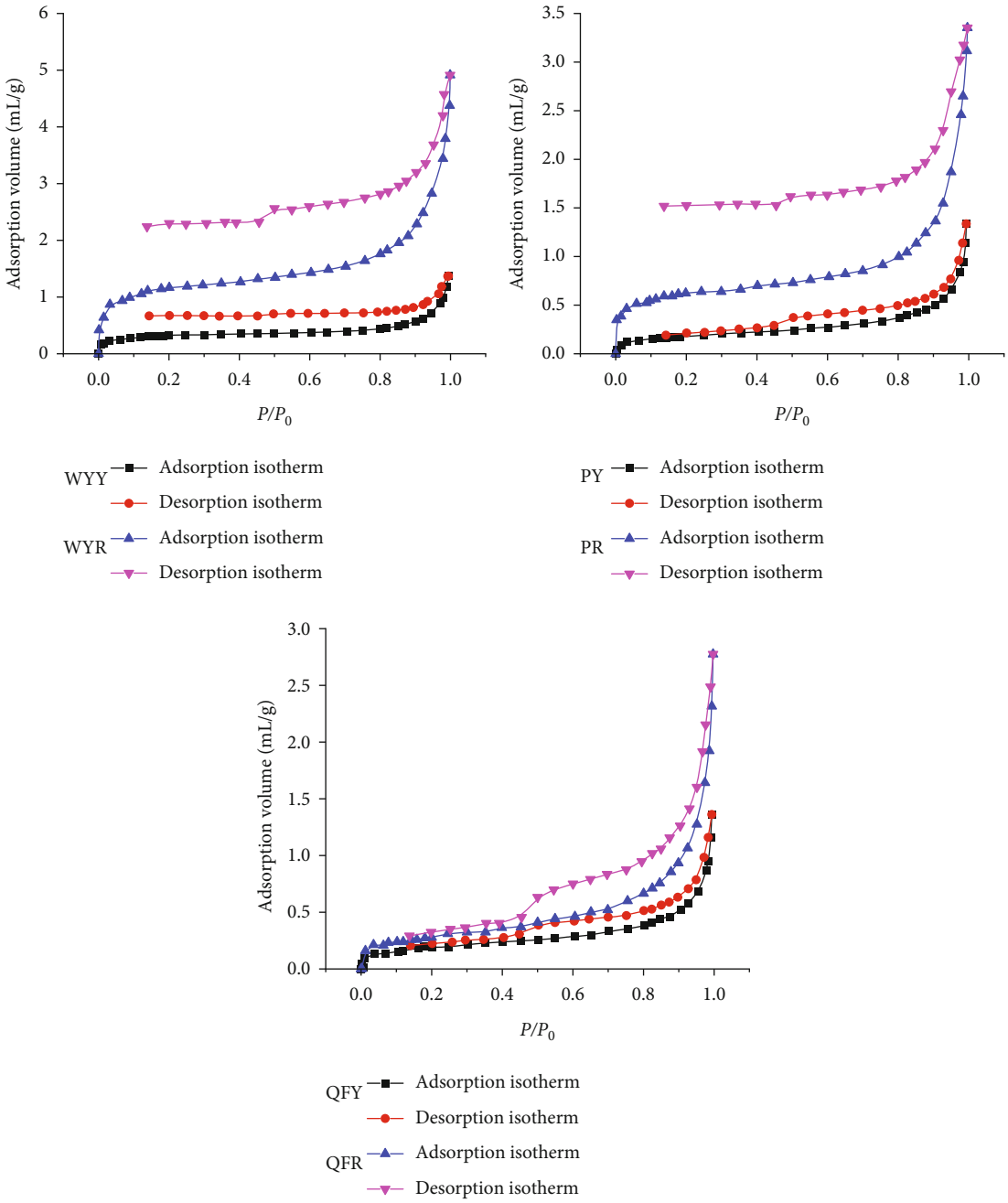

Figure 3: The adsorption/desorption curves of different rank coal samples.

Table 4: Test results of coal samples.

Coal sample	Adsorption capacity (cm^3/g)	Total specific surface area (m^2/g)	Pore volume (cm^3/g)	Average pore diameter (nm)
WYY	1.37001	1.174	0.002713	7.201
WYR	4.91424	4.164	0.007573	7.275
PY	1.33553	0.997	0.002467	10.119
PR	3.35253	1.425	0.005281	13.315
QFY	1.36169	0.701	0.002066	11.791
QFR	2.77532	1.065	0.004302	16.152

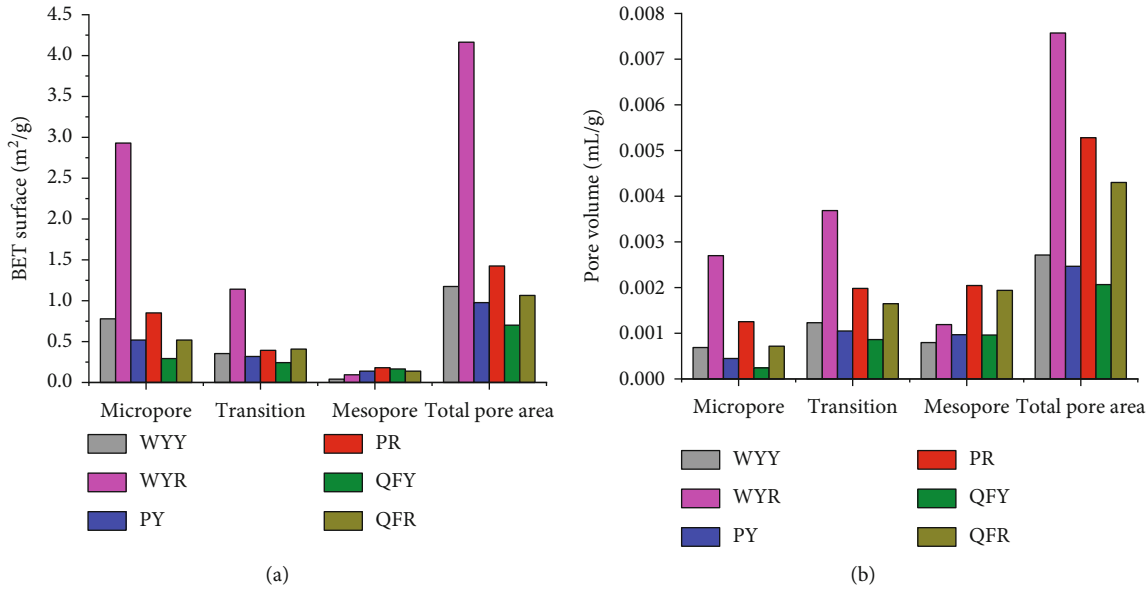

Figure 4: Pore size distribution of coal samples by N_2 adsorption/desorption test: (a) is pore specific surface area and (b) is pore volume of coal samples.

of ln [ln (p_0/p)] and ln V of different coal samples. As shown in Figure 5, the scattered points are not linearly distributed, and the internal pores of the coal samples are divided into two parts, and the relative pressure is calculated, respectively. D_1 represents the fractal dimension that the relative pressure of $p/p_0 < 0.5$ (aperture range is between 2 nm and 10 nm). D_2 represents the pore fractal dimension that the relative pressure of $p/p_0 > 0.5$ (aperture range is larger than 10 nm). The pore fractal dimension results are shown as Table 2. As can be seen from Table 2, the pore fractal dimension of the small pore section, D_1, was between 2.33 and 2.782, the pore fractal dimension of the large pore section, D_2, was between 2.23 and 2.727, and the pore fractal fitting degree of all coal samples were above 90%, indicating that the coal samples with different metamorphism and different destruction types had obvious pore fractal characteristics in the small pores and the large pores. The pore size that N_2 molecules can enter is generally less than 10 nm, and D_1 can be considered to reflect the overall pore structure below 10 nm. Therefore, the fractal dimension D_1 is the focus of the study. As can be seen from Table 2, the fractal dimension D_1 increases with the coal metamorphism, and the soft coal sample is larger than the hard coal sample. The average small pore fractal dimension of different metamorphism coal is shown in Figure 6, indicating that the higher the metamorphism, the larger the small pore fractal dimension, more irregular and more complex pore structures, and the adsorption capacity of the coal is stronger.

3.3. Methane Adsorption Isotherm Results. Methane adsorption in coal sample is a physical adsorption phenomenon, which is caused by Vander Waals forces. The relationship between adsorption content and pressure fits the Langmuir model, and the Langmuir model can be expressed as Equation (3) [40].

$$V = \frac{abP}{1 + bP}, \tag{3}$$

where V is adsorption content, mL/g; a represents the limiting adsorption content of coal samples when the pressure is infinite, mL/g; b is a Langmuir constant describing the intensity of the adsorption energy, MPa^{-1}; and P is the methane pressure, MPa.

The adsorption isotherm curves at different adsorption times of coal samples can be obtained by using the methane adsorption experimental device (Figure 1), and the results are shown in Figure 7. As shown in Figure 7, the methane adsorption content increases with increasing methane pressure and the adsorption time, while the increasing rate is decreasing. Figure 7 shows the adsorption isotherm in good agreement with the Langmuir equation.

The Langmuir constants at different adsorption time of different coal samples are shown in Table 5 and Figure 8. The adsorption capacity of the soft coal is larger than the hard coal, which is consistent with previous studies. As with the adsorption time increasing, the methane adsorption content increases, and the increasing rate of different coal samples are different. The absolute values of the increasing adsorption rate were in the following order: WY > P > QF, namely, the higher the metamorphic degree of coal sample, the higher the increasing rate of adsorption. Take WYY coal sample as an example, the adsorption capacities at the adsorption time of 4 h, 8 h, 12 h, 16 h, 20 h, and 24 h are 32.36 mL/g, 33.67 mL/g, 36.36 mL/g, 38.76 mL/g, 39.53 mL/g, and 40.65 mL/g, respectively. That is, the Langmuir constant a increases with the adsorption time increasing, as shown in Figure 8(a). However, the Langmuir constant b decreases

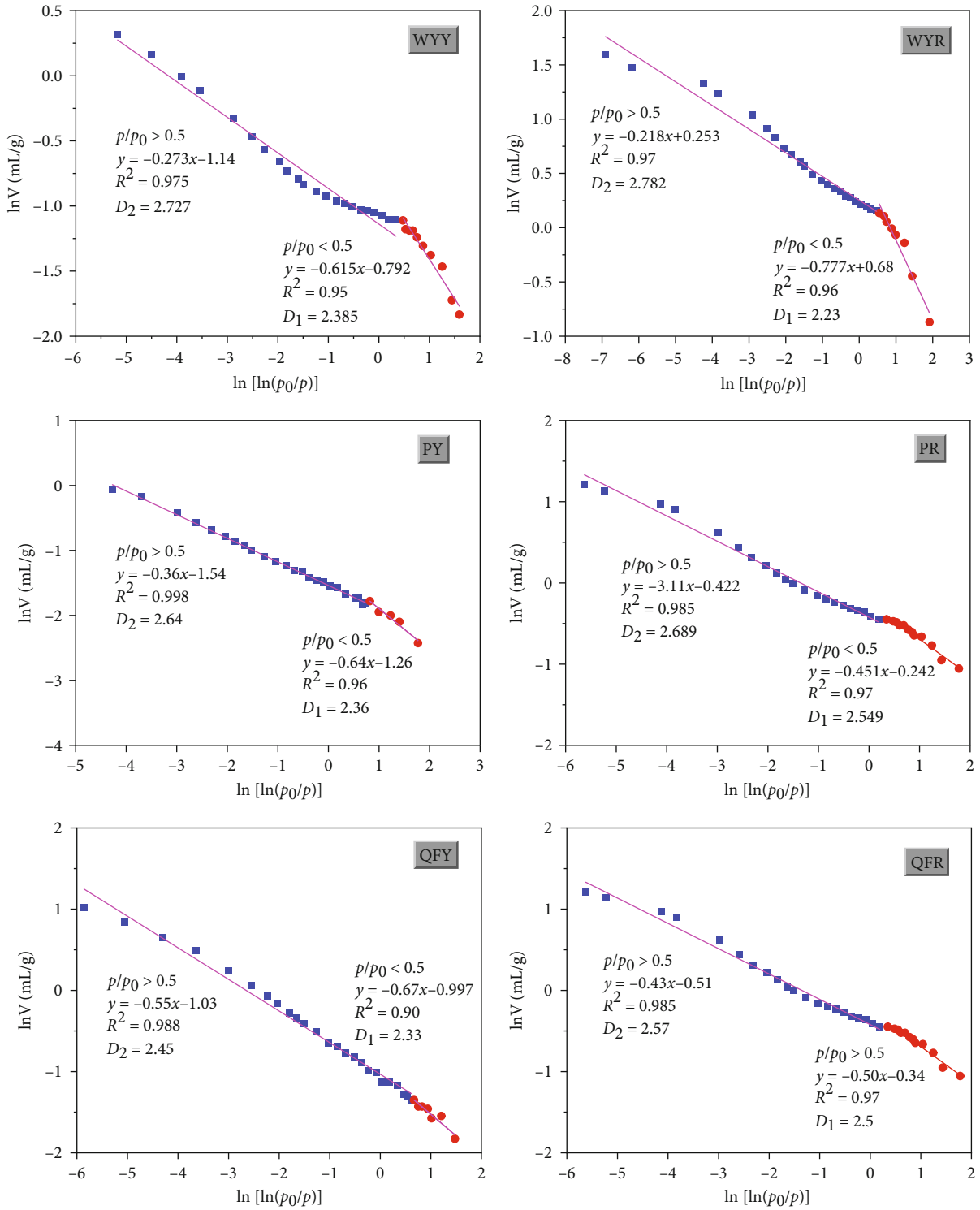

Figure 5: Fractal dimension of coal samples.

with the adsorption time increasing, as shown in Figure 8(b). Take WYY coal sample as an example, the Langmuir constant b at the adsorption time of 4 h, 8 h, 12 h, 16 h, 20 h, and 24 h are 1.57 MPa^{-1}, 1.59 MPa^{-1}, 1.54 MPa^{-1}, 1.53 MPa^{-1}, 1.51 MPa^{-1}, and 1.53 MPa^{-1}, respectively.

As is shown from Table 5, the higher the metamorphic degree of coal sample, the larger the Langmuir a, which order from large to small is WY > P > QF. For the same coal sample, the Langmuir constant a is a variable value at different adsorption time. When the adsorption time exceeds 7 h, the Langmuir constant a is still increasing and gradually tends to be stable with the extension of adsorption time. When the limit of methane adsorption constant is reaching, namely, the Langmuir constant is the maximum, the coal

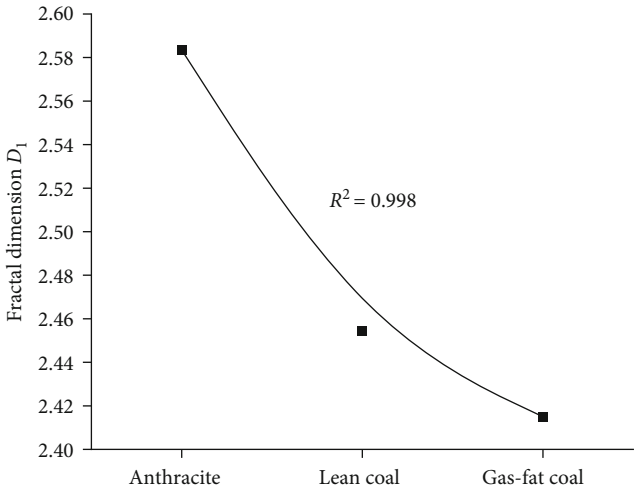

Figure 6: Average small pore fractal dimension of different metamorphism coal.

sample will reach the adsorption equilibrium state. When the coal samples methane reaches adsorption equilibrium, the Langmuir constants a are as follows: WYY is 41.32 mL/g, WYR is 43.29 mL/g, PY is 37.45 mL/g, PR is 40.65 mL/g, QFY is 27.62 mL/g, and QFR is 28.82 mL/g. The Langmuir constant a of soft coal sample is larger than the hard coal sample.

As is shown from Figure 8(b), the Langmuir constant b has a negative exponential function with the adsorption time, which can be expressed as

$$b(t) = \alpha e^{-\beta t}, \tag{4}$$

where $b(t)$ is the Langmuir constant b infected by temperature and coal property, MPa^{-1}; t is the adsorption time, h; α and β are the curve fitting coefficients.

It is noted that the process for coal methane to reach the adsorption equilibrium state is too long, and it is not advisable to extend the adsorption time infinitely to pursue the accuracy of measurement. Therefore, limiting the adsorption time in engineering applications is necessary.

3.4. Effect of Adsorption Time on Coal Seam Methane Content. Coalbed methane (CBM) has two kinds of states: adsorbed state and free state. The adsorbed state usually accounts for more than 80%. The CBM content is not only an indispensable basic parameter for the evaluation of coal seam gas risk degree, the control of gas disaster, and the exploitation and utilization of CBM resources but also a main index for the prediction of coal and gas outburst risk and the test of regional outburst prevention measures. The indirect method is generally used to measure the CBM content, and the Langmuir constants a and b are the basic parameters of indirect method. The CBM content is equal to the sum of free state methane and adsorbed state methane. The free state methane exists in the pores of coal seam or the holes of surrounding rock, and its molecules can move freely and obey the free gas law. According to the gas equation of state (Marott's Law), the amount of free state methane can be expressed as Equation (5). The adsorbed methane content of coal can be expressed as Equation (6), and the methane content of coal seam can be expressed as Equation (7).

$$Q_f = \frac{VPT_0}{TP_0Z}, \tag{5}$$

where Q_f is the free gas quantity of coal sample, mL/g; V is the pore volume per unit mass of coal, m^3/t; P is the methane pressure, MPa; T_0 is the absolute temperature at standard state, ˚C; P_0 is the absolute pressure at standard state, MPa; Z is the compressibility of methane.

$$Q_{ad} = \frac{abP}{1+bP} \times e^{n(t_0-t)} \times \frac{1}{1+0.31M_{ad}} \times \frac{100 - A_{ad} - M_{ad}}{100}, \tag{6}$$

where Q_{ad} is the adsorbed gas content of coal in standard condition, mL/g; a is the Langmuir constant a, mL/g; b is the Langmuir constant b, MPa^{-1}; $n = 0.02/(0.993 + 0.07P)$; t_0 is the experimental temperature, ˚C; t is the coal seam temperature, ˚C; M_{ad} is the moisture of coal sample, %; A_{ad} is the ash content of coal sample, %.

$$Q = \frac{VPT_0}{TP_0Z} + \frac{abP}{1+bP} \times e^{n(t_0-t)} \times \frac{1}{1+0.31M_{ad}} \times \frac{100 - A_{ad} - M_{ad}}{100}, \tag{7}$$

where Q is the CBM content, mL/g.

Table 6 shows the CBM content and numerical percentage of the maximum value at different adsorption time by using the indirect method. The CBM content increases with the extension of adsorption time and tends to be stable gradually in all coal samples. At the same time, the CBM contents were in the following order: WYR > WYY > PR > PY > QFR > QFY; the soft coal samples are larger than hard coal samples. The CBM content of different coal samples are shown in Figure 9. From the curves trend, the CBM content increases with the increase of adsorption time and finally tends to be stable, which conforms to Langmuir model. The Langmuir equation is used to fit the data, and the CBM content under the adsorption equilibrium state can be obtained: 18.38 m^3/t for WYY sample, 21.74 m^3/t for WYR sample, 9.41 m^3/t for PY sample, 10.95 m^3/t for PR sample, 5.96 m^3/t for QFY sample, and 7.62 m^3/t for QFR sample. The higher the metamorphic degree of coal sample is, the longer the adsorption time is needed to reach the equilibrium state of methane adsorption. Coal samples with high metamorphism degree, such as WYY coal and WYR coal, only reach 92.87% and 91.44% of the maximum value when the adsorption time is 24 h, while PY coal and PR coal can reach 96.97% and 94.36% of the maximum value in 20 h; QFY coal and QFR coal reach 96.14% and 94.36% of the maximum value at 4 h adsorption time. For coal samples with different destruction types of the same metamorphic degree, the adsorption time of soft coal is longer than hard

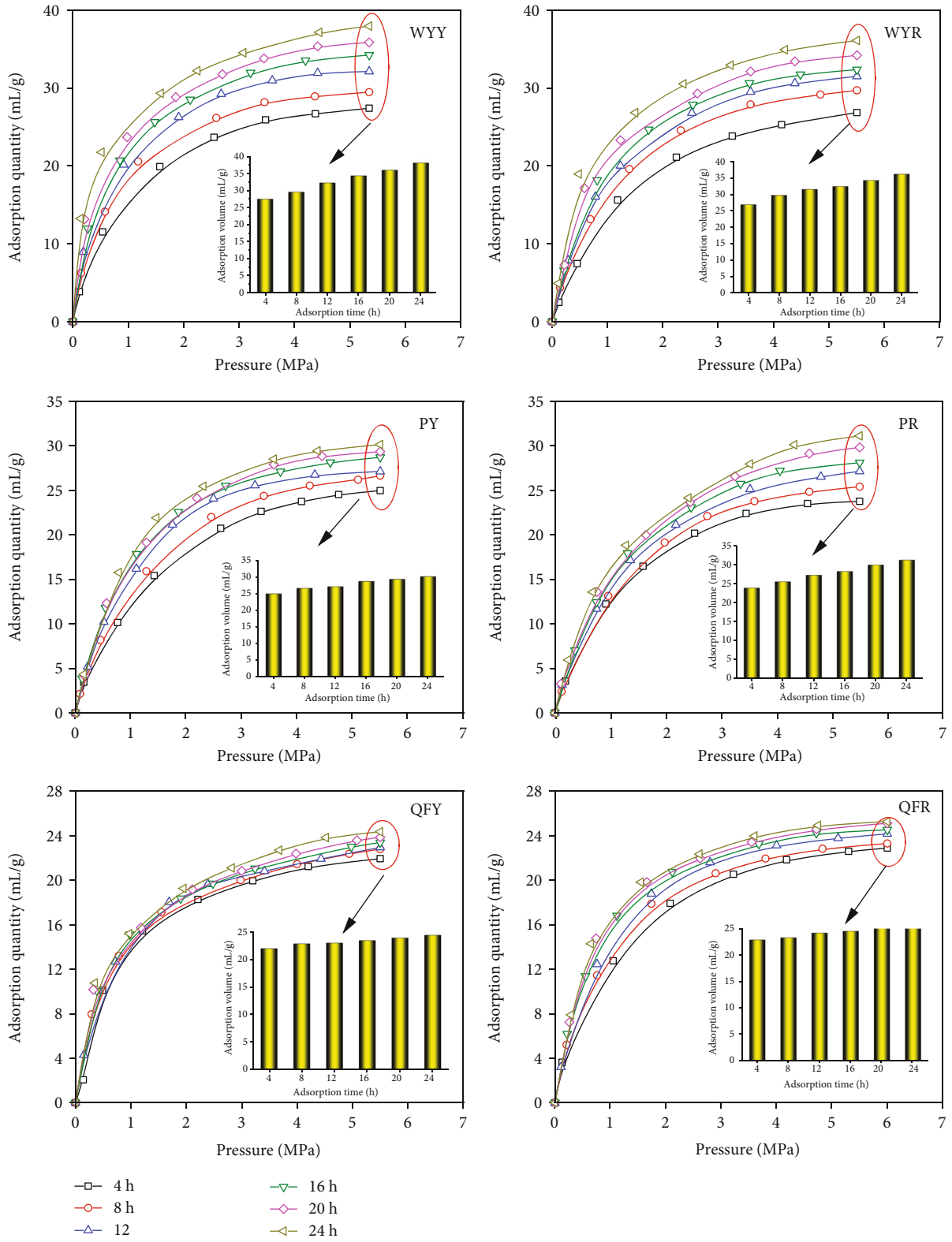

Figure 7: Methane adsorption isotherm at different adsorption times and the fitting Langmuir curves.

coal to reach the equilibrium state of methane adsorption. With the extension of adsorption time, the adsorption of coal methane is closer to the adsorption equilibrium state for the same coal sample under the same conditions. When the adsorption time is 8 h, the CBM content of coal samples with low metamorphism degree, such as QFY coal and QFR coal, has reached 97.65% and 94.75% of the maximum value, respectively, while the gas content of WYY coal is 79.65%,

Table 5: Methane adsorption constants of different coal samples in different adsorption time.

Adsorption time/h	WYY		WYR		PY		PR		QFY		QFR	
	a	*b*	*a*	*b*	*a*	*b*	*a*	*b*	*a*	*b*	*a*	*b*
4	32.36	1.57	34.36	1.21	31.85	1.03	30.58	0.81	24.51	1.41	26.67	1.13
8	33.67	1.59	35.71	1.12	32.79	1.03	32.79	0.79	25.51	1.39	27.17	1.07
12	36.36	1.54	37.59	1.13	33.44	0.95	33.67	0.76	25.84	1.33	27.78	1.05
16	38.76	1.53	38.02	1.08	34.34	0.97	35.97	0.72	26.32	1.37	27.93	1.06
20	39.53	1.51	39.68	1.12	35.84	0.91	36.49	0.69	26.59	1.39	28.01	1.02
24	40.65	1.53	41.67	1.08	36.11	0.93	38.75	0.71	27.11	1.35	28.49	1.03

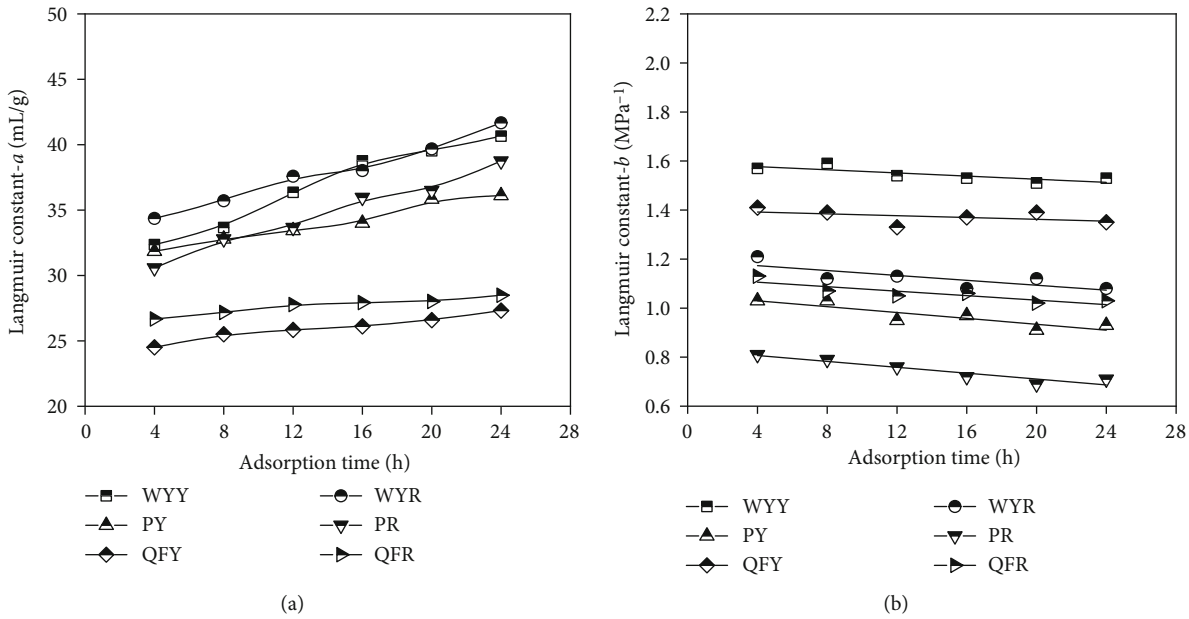

Figure 8: Langmuir constants at different adsorption time: (a) is the Langmuir constant *a*; (b) is the Langmuir constant *b*.

Table 6: CBM content and numerical percentage of the maximum value at different adsorption time.

Adsorption time/h	CBM content (mL·g^{-1})						Numerical percentage CBM content (%)					
	WYY	WYR	PY	PR	QFY	QFR	WYY	WYR	PY	PR	QFY	QFR
4	12.98	14.58	6.78	7.62	5.73	7.19	70.62	67.07	76.01	74.56	96.14	94.36
8	14.64	15.74	7.62	8.15	5.82	7.22	79.65	72.40	85.43	79.75	97.65	94.75
12	15.74	17.41	8.13	8.96	5.86	7.25	85.64	80.08	91.14	87.67	98.32	95.14
16	16.50	18.44	8.24	9.16	5.88	7.37	89.77	84.82	92.38	89.63	98.66	96.72
20	16.89	19.26	8.65	9.82	5.90	7.47	91.89	88.59	96.97	96.09	98.99	98.03
24	17.07	19.88	8.84	10.14	5.92	7.53	92.87	91.44	99.10	99.22	99.33	98.82

Note: numerical percentage CBM content is the CBM content at different adsorption times divided by CBM content at adsorption equilibrium state.

WYR coal is 72.40%, PY coal is 85.43%, and PR coal is 79.75%. It indicates that adsorption time of 8 h cannot guarantee that all coal samples can reach adsorption equilibrium state.

3.5. Discussion on Reasonable Adsorption Time. The coal adsorbing methane is a comprehensive process of seepage and diffusion. The seepage is caused by methane pressure gradient in large pore system, and methane concentration gradient causes diffusion in microporous system. Methane molecules percolate and diffuse into the coal body until adsorption equilibrium is reached.

The methane adsorption saturation is the fundamental reason that affects the Langmuir constant *a*. In the adsorption process, the influence of adsorption time on methane adsorption saturation can be divided into three stages. The unsaturation of adsorbed methane in coal body is very large at the initial stage of adsorption process; the adsorption

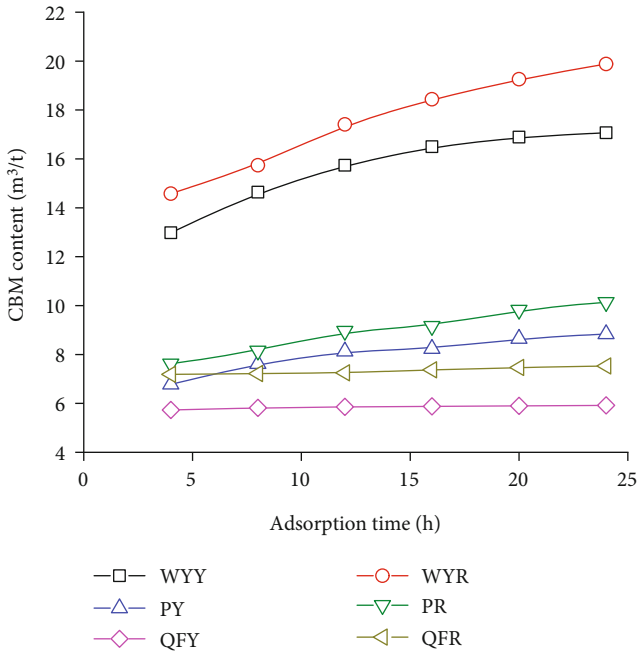

Figure 9: CBM content of different coal samples.

speed is extremely fast under the action of pressure gradient and concentration gradient. The amount of methane adsorption increases gradually when the pressure gradient and concentration gradient in the coal body decrease gradually, and the gas diffusion rate and the coal adsorption rate of methane decrease continuously, the adsorption saturation under the corresponding adsorption pressure increases. Then, the pressure gradient and concentration gradient in the coal tended to be 0, the coal adsorption of methane gradually tends to saturation state, the gas diffusion rate and the coal's methane adsorption rate attenuated to 0, and the gas adsorption quantity did not increase with the increase of the adsorption time. At this point, the coal body reached the gas adsorption equilibrium state. Therefore, with the extension of adsorption time, the methane adsorption constant a will gradually increase and tend to be a stable value in the test process [41–43].

The rich pores in coal samples are developed, the pore volume and specific surface area increase with the degree of coal metamorphism, and micropore increases the difficulty of the methane molecules entering the micropore by extending the methane migration channel, lower permeability. In addition, the methane molecules must overcome the surface tension of the pores and cracks before entering the microporous cracks. The more complex the pore structure of coal is, the greater the force that the methane molecules need to overcome is, which also reduces the migration intensity of methane molecules and thus increases the time required by coal for methane saturation adsorption. Therefore, the coal sample has not reached the true adsorption equilibrium state, but is in a false equilibrium when the adsorption time is far less than the adsorption equilibrium time. At this point, if the adsorption time continues to be extended, the gas adsorption amount will continue to increase, and the Langmuir a will continue to increase.

Table 7: Langmuir constants a and b at reasonable adsorption time.

Coal samples	Reasonable adsorption time/h	a/(mL/g)	b/(MPa^{-1})
WYY	25	41.56	1.51
WYR	28	42.95	1.04
PY	18	35.04	0.94
PR	22	38.64	0.71
QFY	7	25.43	1.38
QFR	8	27.21	1.07

It takes a long time for coal to reach the adsorption equilibrium state to ensure the coal sample to reach the adsorption equilibrium state. The test result with high accuracy can be obtained by extending the adsorption time infinitely, which will increase the testing period and cost of the adsorption constant. Therefore, the reliability of the measured values and the economy in engineering application must be considered comprehensively, that is, the reasonable adsorption equilibrium time of coal samples must be determined.

In engineering applications, the reliability of the measured values should meet more than 85%. 200 sample sizes with a confidence of 85% are selected to investigate the reasonable adsorption equilibrium time of WYY, WYR, PY, PR, QFY, and QFR within 1-200 h. From the definition of the confidence interval, the confidence interval $[\theta_1,\theta_2]$ is satisfied as

$$[\theta_1, \theta_2] = \left[\bar{x} - t_{\alpha/2}\frac{\sigma}{\sqrt{n}}, \bar{x} + t_{\alpha/2}\frac{\sigma}{\sqrt{n}}\right], \quad (8)$$

where n is sample size; $\bar{x}$ is sample average, mL/g; σ^2 is sample variance; and α is confidence coefficient, %.

According to relevant calculation, the mean sampling error is 0.3312 mL/g, the degree of freedom is 199, the bilateral quantile of t distribution is 1.445, and the allowable error is 0.479 mL/g. Therefore, the Langmuir a is 41.56 mL/g, the corresponding reasonable adsorption time is 25 h, and the Langmuir b is 1.51 MPa^{-1}. Similarly, other coal samples are solved according to the above method, and the results are shown in Table 7. The reasonable adsorption time increases with increasing the coal ranks. This is because the higher the degree of coal rank, the larger of the pore volume, the larger of the specific surface area, the more developed of the micropores, the higher the reasonable adsorption time, then the higher the Langmuir constant a. The reasonable adsorption time increases with increasing the coal destruction type, namely, the reasonable adsorption time of soft coal is larger than the hard coal. The reasons are that the pore volume, specific surface area, and the proportion of micropores of soft coal are larger than the hard coal, resulting in the increasing of adsorption capacity. As the coal methane adsorption process is exothermic reaction, the temperature of coal sample increases, and the Langmuir constant b tends

to decrease. Above all, the reasonable adsorption time of coal samples are as follows: WYY is 25 h, WYR is 28 h, PY is 18 h, PR is 22 h, QFY is 7 h, and QFR is 8 h.

4. Conclusion

In this paper, the pore structural parameters of coal samples with different coal ranks and destruction types were measured by mercury intrusion test and N_2 adsorption/desorption test. The adsorption characteristics of coal samples and the coalbed methane content for different adsorption time were studied by methane isothermal adsorption test. The results show the following:

(1) The specific surface area and the total pore volume increase correspondingly with increasing destruction type for the same coal rank. The fractal dimension of N_2 adsorption test increases with increasing the coal metamorphism

(2) Adsorption time is one of the important factors affecting the Langmuir constants. The longer the adsorption time is, the closer saturation state of the coal methane adsorption is, and the larger of coal methane adsorption capacity and Langmuir constant *a* are. However, due to the coal methane adsorption process is exothermic reaction, the temperature of coal sample increases, and the Langmuir constant *b* tends to decrease

(3) The measurement of the coalbed methane (CBM) content of the coal seam is affected by the influence of adsorption time to the Langmuir constants. The higher the metamorphic degree of coal sample is, the longer the adsorption time is needed to reach the equilibrium state of methane adsorption, and the adsorption equilibrium time of soft coal is longer than hard coal

(4) Under the condition that the reliability of the measured value is 85%, the reasonable adsorption times of coal samples are 28 h for anthracite, 22 h for lean coal, and 8 h for gas-fat coal

Data Availability

The (data type) data used to support the findings of this study are included within the article.

Conflicts of Interest

The authors declare no competing interests.

Authors' Contributions

Qiao Wang conceived the experiment and analyzed the results; Zhaofeng Wang, Jiwei Yue, Liguo Wang, Jiaxin Dong, and Ronghui Tan coordinated the study and helped draft the manuscript. All authors gave final approval for publication.

Acknowledgments

This work was financially supported by the National Natural Science Foundation of China (nos. 52074107 and 52174172), the scientific research start-up fund for high-level talent introduction of Anhui University of Science and Technology (2021yjrc45), and the Key Natural Science Research Projects of Colleges and Universities in Anhui Province.

References

[1] W. P. Diamond and S. J. Schatzel, "Measuring the gas content of coal: a review," *International Journal of Coal Geology.*, vol. 35, no. 1-4, pp. 311–331, 1998.

[2] X. L. Li, Z. Y. Cao, and Y. L. Xu, "Characteristics and trends of coal mine safety development," *Energy Sources, Part A: Recovery, Utilization, and Environmental Effects.*, vol. 12, pp. 1–19, 2020.

[3] T. A. Moore, "Coalbed methane: a review," *International Journal of Coal Geology.*, vol. 101, no. 1, pp. 36–81, 2012.

[4] S. Tao, Z. J. Pan, S. L. Tang, and S. Chen, "Current status and geological conditions for the applicability of CBM drilling technologies in China: a review," *International Journal of Coal Geology.*, vol. 202, pp. 95–108, 2019.

[5] X. Li, S. Chen, E. Wang, and Z. Li, "Rockburst mechanism in coal rock with structural surface and the microseismic (MS) and electromagnetic radiation (EMR) response," *Engineering Failure Analysis*, vol. 124, no. 6, article 105396, 2021.

[6] Z. Jarosław, F. Piotr, and B. Henryk, "Estimation of methane content in coal mines using supplementary physical measurements and multivariable geostatistics," *International Journal of Coal Geology*, vol. 118, pp. 33–44, 2013.

[7] F. K. Wang, X. S. Zhao, Y. P. Liang, X. L. Li, and Y. L. Chen, "Calculation model and rapid estimation method for coal seam gas content," *Processes*, vol. 6, no. 11, p. 223, 2018.

[8] T. Liu, B. Q. Lin, X. H. Fu et al., "Experimental study on gas diffusion dynamics in fractured coal: a better understanding of gas migration in in-situ coal seam," *Energy*, vol. 195, article 117005, 2020.

[9] N. Szlązak, D. Obracaj, and M. Korzec, "Estimation of gas loss in methodology for determining methane content of coal seams," *Energies*, vol. 14, no. 4, p. 982, 2021.

[10] S. Tao, S. D. Chen, and Z. J. Pan, "Current status, challenges, and policy suggestions for coalbed methane industry development in China: a review," *Energy Science & Engineering*, vol. 7, pp. 1–16, 2019.

[11] X. Li, S. Chen, Q. Zhang, X. Gao, and F. Feng, "Research on theory, simulation and measurement of stress behavior under regenerated roof condition," *Geomechanics and Engineering*, vol. 26, no. 1, pp. 49–61, 2021.

[12] Z. B. Yang, Y. Qin, W. ZhaoFeng, Z. F. Wang, W. Geoff, and C. F. Wu, "Desorption-diffusion model and lost gas quantity estimation of coalbed methane from coal core under drilling fluid medium," *Science China-Earth Sciences*, vol. 53, no. 4, pp. 626–632, 2010.

[13] H. J. Xu, F. Ahmad, B. L. Hu et al., "Methodology for lost gas determination from exploratory coal cores and comparative evaluation of the accuracy of the direct method," *ACS Omega*, vol. 6, no. 30, pp. 19695–19704, 2021.

[14] J. H. Levy, S. J. Day, and J. S. Killingley, "Methane capacities of Bowen Basin coals related to coal properties," *Fuel*, vol. 76, no. 9, pp. 813–819, 1997.

[15] Y. P. Chen and Z. J. Pan, "Reservoir properties of Chinese tectonic coal: a review," *Fuel*, vol. 260, article 116350, 2020.

[16] R. Sakurovs, S. Day, S. Weir, and G. Duffy, "Temperature dependence of sorption of gases by coals and charcoals," *International Journal of Coal Geology*, vol. 73, no. 3-4, pp. 250–258, 2008.

[17] W. Guo, W. Xiong, S. S. Gao, Z. M. Hu, H. L. Liu, and R. Z. Yu, "Impact of temperature on the isothermal adsorption/desorption of shale gas," *Petroleum Exploration and Development*, vol. 40, no. 4, pp. 514–519, 2013.

[18] X. Tang, Z. Q. Li, N. Ripepi, A. K. Louk, Z. F. Wang, and D. Y. Song, "Temperature-dependent diffusion process of methane through dry crushed coal," *Journal of Natural Gas Science and Engineering*, vol. 22, pp. 609–617, 2015.

[19] Z. F. Wang, X. Tang, G. W. Yue, B. Kang, C. Xe, and X. J. Li, "Physical simulation of temperature influence on methane sorption and kinetics in coal: benefits of temperature under 273.15 K," *Fuel*, vol. 158, no. 10, pp. 207–216, 2015.

[20] C. Guan, S. M. Liu, C. W. Li, Y. Wang, and Y. X. Zhao, "The temperature effect on the methane and CO_2 adsorption capacities of Illinois coal," *Fuel*, vol. 211, no. 1, pp. 241–250, 2018.

[21] Y. Liu, Y. M. Zhu, S. M. Liu, W. Li, and X. Tang, "Temperature effect on gas adsorption capacity in different sized pores of coal: experiment and numerical modeling," *Journal of Petroleum Science and Engineering*, vol. 165, no. 6, pp. 821–830, 2018.

[22] S. Y. Liu, C. H. Wei, W. C. Zhu, and M. Zhang, "Temperature- and pressure-dependent gas diffusion in coal particles: numerical model and experiments," *Fuel*, vol. 266, no. 4, article 117054, 2020.

[23] S. M. Liu, X. L. Li, D. K. Wang, and D. Zhang, "Experimental study on temperature response of different ranks of coal to liquid nitrogen soaking," *Natural Resources Research.*, vol. 30, no. 2, pp. 1467–1480, 2021.

[24] J. I. Joubert, C. T. Grein, and D. Bienstock, "Effect of moisture on the methane capacity of American coals," *Fuel*, vol. 53, no. 3, pp. 186–191, 1974.

[25] C. R. Clarkson and R. M. Bustin, "Binary gas adsorption/desorption isotherms: effect of moisture and coal composition upon carbon dioxide selectivity over methane," *International Journal of Coal Geology.*, vol. 42, no. 4, pp. 241–271, 2000.

[26] M. Y. Chen, Y. P. Cheng, H. R. Li, L. Wang, K. Jin, and J. Dong, "Impact of inherent moisture on the methane adsorption characteristics of coals with various degrees of metamorphism," *Journal of Natural Gas Science and Engineering.*, vol. 55, pp. 312–320, 2018.

[27] X. Song, X. X. Lv, Y. Q. Shen, S. Guo, and Y. Guan, "A modified supercritical Dubinin–Radushkevich model for the accurate estimation of high pressure methane adsorption on shales," *International Journal of Coal Geology*, vol. 193, pp. 1–15, 2018.

[28] T. Xu, R. Nino, P. S. Nicholas, and Y. Lingjie, "Thermodynamic analysis of high pressure methane adsorption in Longmaxi shale," *Journal Article*, vol. 193, pp. 411–418, 2017.

[29] J. Yue, Z. Wang, J. Chen, M. Zheng, Q. Wang, and X. Lou, "Investigation of pore structure characteristics and adsorption characteristics of coals with different destruction types," *Adsorption Science & Technology*, vol. 37, no. 7-8, pp. 623–648, 2019.

[30] F. Zhao, Q. Sun, and W. Q. Zhang, "Fractal analysis of pore structure of granite after variable thermal cycles," *Environmental Earth Sciences*, vol. 78, no. 24, p. 677, 2019.

[31] X. X. He, Y. P. Cheng, B. Hu, C. H. Wang, M. H. Yi, and L. Wang, "Effects of coal pore structure on methane-coal sorption hysteresis: An experimental investigation based on fractal analysis and hysteresis evaluation," *Fuel*, vol. 269, article 117438, 2020.

[32] L. L. Qi, X. Tang, Z. F. Wang, and X. S. Peng, "Pore characterization of different types of coal from coal and gas outburst disaster sites using low temperature nitrogen adsorption approach," *International Journal of Mining Science and Technology*, vol. 27, no. 2, pp. 371–377, 2017.

[33] M. Zhang and X. H. Fu, "Characterization of pore structure and its impact on methane adsorption capacity for semi-anthracite in Shizhuangnan block, Qinshui Basin," *Journal of Natural Gas Science and Engineering*, vol. 60, pp. 49–62, 2018.

[34] Q. Wei, X. Q. Li, J. Z. Zhang et al., "Full-size pore structure characterization of deep-buried coals and its impact on methane adsorption capacity: a case study of the Shihezi formation coals from the Panji deep area in Huainan coalfield, southern North China," *Journal of Petroleum Science and Engineering*, vol. 173, pp. 975–989, 2019.

[35] P. Zhejun and D. C. Luke, "Modelling permeability for coal reservoirs: a review of analytical models and testing data," *Journal Article*, vol. 92, pp. 1–44, 2012.

[36] W. Zhao, Y. P. Cheng, M. Yuan, and F. H. An, "Effect of adsorption contact time on coking coal particle desorption characteristics," *Energy & Fuels*, vol. 28, no. 4, pp. 2287–2296, 2014.

[37] A. G. Paithankar and G. B. Misra, "A critical appraisal of the protodyakonov index," *International Journal of Rock Mechanics & Mining Sciences & Geomechanics Abstracts*, vol. 13, no. 8, pp. 249–251, 1976.

[38] S. Zhao, X. J. Chen, X. J. Li, L. L. Qi, and G. X. Zhang, "Experimental analysis of the effect of temperature on coal pore structure transformation," *Fuel*, vol. 305, article 121613, 2021.

[39] J. W. Yue, Z. F. Wang, B. M. Shi, J. Dong, and X. Shen, "Interaction mechanism of water movement and gas desorption during spontaneous imbibition in gas-bearing coal," *Fuel*, vol. 318, article 123669, 2022.

[40] W. Zhao, K. Wang, C. W. Li et al., "Analysis on the accuracy of laboratory measurement of apparent diffusion coefficient of adsorbed gas in matrix based on the competition relationship between gas flow and gas diffusion," *Journal of China Coal*, vol. 2, pp. 1–11, 2020.

[41] W. Zhao, Y. P. Cheng, Z. Pan, K. Wang, and S. Liu, "Gas diffusion in coal particles: a review of mathematical models and their applications," *Fuel*, vol. 252, pp. 77–100, 2019.

[42] Z. Lou, K. Wang, J. Zang, W. Zhao, B. Qin, and T. Kan, "Effects of permeability anisotropy on coal mine methane drainage performance," *Journal of Natural Gas Science and Engineering*, vol. 86, p. 103733, 2021.

[43] H. Zhang, Y. G. Zhang, D. J. Lei, and Y. Jiao, "Characterization of structure of kaolinite in tectonically deformed coal: evidence of mechanochemistry," *Energy Sources Part A Recovery Utilization and Environmental Effects*, vol. 5, pp. 1–12, 2021.